Cancer Research

53BP1 Is a Haploinsufficient Tumor Suppressor and Protects Cells from Radiation Response in Glioma

Massimo Squatrito[1,5], Fabio Vanoli[2], Nikolaus Schultz[3], Maria Jasin[2], and Eric C. Holland[1,4,5]

Abstract

The DNA damage response (DDR) plays a crucial role in tumor development in different tissues. Here, we show that p53-binding protein 1 (53BP1), a key element of the DDR, is heterozygously lost in approximately 20% of human glioblastoma multiforme (GBM) specimens, primarily of the Proneural subtype, and low 53BP1 expression levels are associated with worse prognosis. We present evidence that 53BP1 behaves as haploinsufficient tumor suppressor in a mouse model of platelet-derived growth factor–induced gliomagenesis. We also show that very low level of 53BP1 as found in 53BP1 null gliomas or robust *53BP1* gene silencing in glioma cell lines (but not 53BP1 heterozygous tumors or partial gene knockdown) sensitizes glioma cells to ionizing radiation (IR), both *in vitro* and *in vivo*. We further show the *53BP1* gene silencing induces defects in the nonhomologous end-joining (NHEJ) DNA repair pathway. These deficiencies lead to a failure to fully repair the damaged DNA upon exposure of glioma cells to IR with a consequent prolonged cell-cycle arrest and increased apoptosis. Our data suggest that either 53BP1 or other NHEJ components may be critical molecules to be pharmacologically targeted in GBM in combination with standard therapies. *Cancer Res; 72(20); 5250–60. ©2012 AACR.*

Introduction

The p53-binding protein 1 (53BP1) was initially identified as a protein that interacts with the DNA-binding domain of wild-type but not mutant p53, having the ability to modulate p53-mediated transcription activation (1, 2). 53BP1 has subsequently been shown to also have p53-independent functions as a key mediator of the DNA-damage response (DDR) and a direct modulator of DNA double-strand break (DSB) repair (3). 53BP1-deficient cells exhibit increased genomic instability and consequently 53BP1 null mice are highly radiation sensitive, display growth retardation and are tumor prone (4, 5).

Even though a critical role of the DDR pathway in tumor formation and modulation of therapeutic response has been established recently, it is unclear whether 53BP1 takes an active part in these processes, and if so in which tumor type. Here, we show that 53BP1 is frequently heterozygously lost in glioblastoma multiforme (GBM) and behaves as a haploinsufficient tumor suppressor in a mouse model of glioma. Gliomas are the most frequent primary malignancies in the central nervous system (CNS), with GBM being the most malignant form of gliomas. We have previously shown that some essential components of the DDR, such as ATM, Chk2, and p53, are frequently inactivated in GBM and exert a crucial activity during in glioma development and radiation response (6). Contrasting with its role as a tumor suppressor when partly lost, complete loss of 53BP1 in glioma cells increases radiosensitivity both *in vitro* and *in vivo*. We present evidence that the radiation sensitivity might be related to 53BP1 role in modulating nonhomologous end-joining (NHEJ) DNA repair.

Authors' Affiliations: Departments of [1]Cancer Biology and Genetics, [2]Developmental Biology, [3]Computational Biology, [4]Surgery (Neurosurgery), and [5]Brain Tumor Center, Memorial Sloan-Kettering Cancer Center, New York, New York

Note: Supplementary data for this article are available at Cancer Research Online (http://cancerres.aacrjournals.org/).

Corresponding Authors: Massimo Squatrito, 408 E69th Street, New York, NY 10021. Phone: 646-888-2056; Fax: 646-422-0231. E-mail: squatrim@mskcc.org; and Eric C. Holland, E-mail: hollande@mskcc.org

doi: 10.1158/0008-5472.CAN-12-0045

Material and Methods

TCGA analysis

The analysis of the The Cancer Genome Atlas (TCGA) dataset for GBM was conducted through the cBio Cancer Genomics Portal (7), based on the January 24, 2012 Broad Firehose run of TCGA data. Copy number alterations (CNA), expression and survival data of patients are also presented in Supplementary Tables S1 and S2.

Mice and generation of murine gliomas

53bp1$^{-/-}$ mice (4) were obtained from Titia de Lange. Athymic Nude-*Foxn1*^{nu} mice were purchased from Harlan Laboratories. Nestin-tv-a (*Ntv-a*) mice, and procedures for RCAS-mediated gliomagenesis have been described previously (8). All animal experiments were done in accordance with protocols approved by the Institutional Animal Care and Use Committee of Memorial Sloan-Kettering Cancer Center and followed NIH guidelines for animal welfare.

Histology, immunohistochemistry, and TUNEL assay

Tissues were fixed in 10% neutral-buffered formalin and subsequently embedded in paraffin, following standard procedures. Immunohistochemical and terminal deoxynucleotidyl transferase–mediated dUTP nick end labeling (TUNEL)

staining was conducted using a Discovery XT automated staining processor (Ventana Medical Systems, Inc.). The antibodies were diluted in PBS 2% bovine serum albumin as follow: anti-53bp1 (Novus, #NB100-304) 1:800 antiphospho-histone H3 (Ser10; Millipore, #06-750) 1:800. The TUNEL assay was conducted with a terminal transferase recombinant kit (Roche, #333-574-001). The quantification of TUNEL staining was conducted as previously described (6). 53BP1 staining was quantified using the ImageJ software.

Cell culture, transfection, and gene silencing

DF1 cells [American Type Culture Collection (ATCC)] were grown at 39°C in Dulbecco's Modified Eagle's Medium (ATCC) containing 10% FBS (PAA, The Cell Culture Company). U87, U251, and T98G were grown at 37°C in Dulbecco's Modified Eagle's Medium containing 10% FBS. The cell lines used in the manuscript have not been tested or authenticated. DF1 cells were transfected with the RCAS–PDGF viral plasmid, using Fugene 6 Transfection reagent (Roche), accordingly to manufacture protocol. pGIPZ lentiviral *53bp1* shRNAmirs were purchased from Openbiosystem (clone ID and sequences are provided in Supplementary Material and Methods). pRetroSuper retroviral vectors encoding *53bp1* short hairpin RNA (shRNA; 53bp1_A, 5′-GATACTGCCTCATCACAGT-3′; 53bp1_B 5′-GAACGAGGAGACGGTAATA-3′; ref. 9) were kindly provided by Roderik Beijesbergen. Either empty pRetroSuper or pRetroSuper encoding *GFP* shRNA were used as control. Retroviral and lentiviral vectors were introduced into glioma cell lines using standard infection procedures.

More detailed Materials and Methods can be found in Supplementary Materials and Methods.

Results

53BP1 is heterozygously lost in human GBMs, primarily of the Proneural subtype

We conducted an analysis of TCGA dataset for GBM (10) looking at 53BP1 CNAs, mRNA expression levels and protein expression levels. Genomic loss of a single copy of 53BP1 was found in 17.5% (88/501) of GBM samples (Supplementary Table S1). In a subset of this TCGA dataset for which mRNA or protein expression data were available, copy number loss was associated with significantly lower gene expression ($P < 0.0001$, *t* test; Fig. 1A and Supplementary Table S1) and also lower 53BP1 protein levels ($P = 0.006$, *t* test), as measured by reverse phase protein array (RPPA; Fig. 1B and Supplementary Table S1). Patients with lower level of 53BP1 (normalized log 2 mRNA expression < -1) have a poorer survival than patients with higher level of 53BP1 (normalized log 2 mRNA expression > -1; $P = 0.0910$, log-rank Mantel–Cox test and $P = 0.0297$, Gehan–Breslow–Wilcoxon test; Fig. 1C). Analogously, patients with lower 53BP1 RPPA score have a poorer survival than patients with higher 53BP1 RPPA score ($P = 0.0540$, log-rank Mantel–Cox test and $P = 0.0413$, Gehan–Breslow–Wilcoxon test; Supplementary Fig. S1A). We then determined whether 53BP1 CNAs were more common in a specific GBM subtype (11, 12), and we found that loss of 53BP1 is significantly associated with the Proneural subclass ($P < 0.0001$, Fisher exact test). Approximately 35% of the Proneural GBMs (42 of 123) present single copy loss, as compared with the 11% (46 of 412) of nonProneural tumors (Fig. 1D and E and Supplementary Table S1). Moreover, when the patients were stratified accordingly to the different GBM subtypes, low level of 53BP1 were associated with significant worse prognosis ($P = 0.0081$, log-rank Mantel–Cox test) exclusively in the Proneural subclass (Fig. 1F).

53BP1 cooperates with TP53 in tumor suppression, and the loss of one or both copies of 53BP1 greatly accelerates lymphomagenesis in a p53-null mouse model (4, 5). Consequently, we analyzed the TCGA GBM dataset for the co-occurrence of *53BP1* gene copy loss and TP53 alterations (either gene copy loss or somatic mutations). There is a significant co-occurrence of 53BP1 and p53 alterations ($P < 0.0001$, Fisher exact test), but not with MDM2 or MDM4 amplifications, both well-described p53 inhibitors. Approximately 50% (47 of 93) of the patients with one *53BP1* gene copy also present alterations in p53 (Fig. 1D and G; Supplementary Fig. S1B and S1C; Supplementary Table S2), suggesting that 53BP1 might work in p53-indipendent manner in the gliomagenesis process.

53bp1 is a haploinsufficient tumor suppressor in a glioma mouse model

The frequent loss of 53BP1 in human GBMs suggested a putative tumor suppressor activity of this molecule in gliomas. Hence, to directly show a role of 53BP1 loss in glioma formation, we took advantage of the RCAS/tv-a system, which uses a specific avian leukosis virus (RCAS) to mediate gene transfer into somatic cells transgenic for its receptor (tv-a). In this study, we used the *Ntv-a* mice that express the tv-a receptor under the control of the Nestin promoter, a marker of neural/glial stem and progenitor cells (13). Newborn mice were injected with cells producing the RCAS retroviruses carrying the platelet-derived growth factor-B (PDGFB; ref. 14).

In *Ntv-a* mice, loss of either one or both copies of *53bp1* similarly accelerates PDGF-induced glioma formation, with the wild-type mice having an average survival of 105 days, $53bp1^{-/-}$ mice of 59.5 days ($P = 0.0255$, log-rank test) and $53bp1^{+/-}$ of 62 days ($P = 0.0470$, log-rank test; Fig. 2A). Loss of heterozygosity (LOH) was not detected in $53bp1^{+/-}$ gliomas (Fig. 2B). Expression of 53BP1 protein, as measured by immunohistochemistry (IHC), seems to be lower in $53bp1^{+/-}$ gliomas as compared with wild-type tumors, but was still detectable as shown in Fig. 2C, suggesting that *53bp1* might behave as a classic haploinsufficient tumor suppressor gene.

Robust *53BP1* knockdown improves the response to DNA damaging therapy in GBM cells

53BP1 plays a well-established role in the DDR. Therefore, we determined whether gliomas of different *53bp1* genotype presented alterations in radiation sensitivity *in vivo*. Glioma-bearing mice were exposed to 10 Gy ionizing radiation (IR) and apoptosis was measured after 24 hours. Upon treatment with IR $53bp1^{-/-}$ but not $53bp1^{+/-}$ gliomas exhibited a significant increase of TUNEL-positive cells as compared with that seen for wild-type tumors ($P < 0.05$, Student *t* test; Fig. 3A). Analogously, when we exposed to IR normal primary brain cultures derived from pups from the different genotypes, only $53bp1^{-/-}$ and not $53bp1^{+/-}$ cells presented an increased frequency

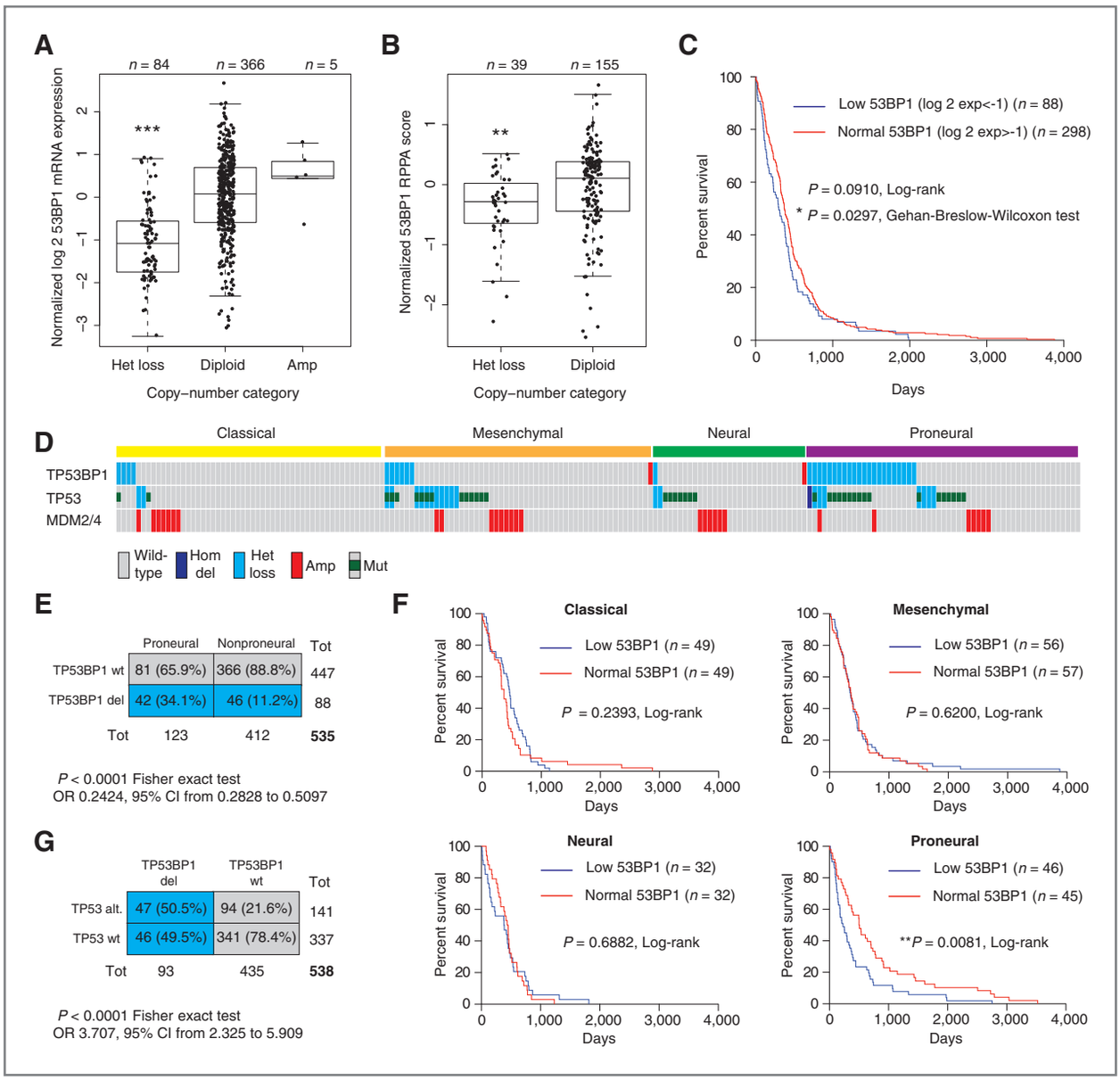

Figure 1. 53BP1 is heterezygously lost in human GBM, primarily of the Proneural subtype, and co-occurs with TP53 alterations. A, CNAs and mRNA expression of TP53BP1 in the TCGA dataset of human GBMs (***, $P < 0.0001$, *t* test). Expression data are normalized on the average expression of diploid samples. B, 53BP1 protein expression measured by RPPA (**, $P = 0.006$, *t* test). C, Kaplan–Meier survival curve of patients with GBM with low (normalized log 2 < −1) and normal/high (normalized log 2 > −1) 53BP1 mRNA expression. D, gene-dosage profiles for TP53BP1, TP53, and MDM2/4 across 191 GBMs in TCGA dataset, separated accordingly to the 4 molecular subtypes of glioblastoma (Classical, Mesenchymal, Neural, and Proneural). E, 2-way contingency table showing that TP53BP1 copy loss is significantly associated with the Proneural subtype. F, Kaplan–Meier survival curve of patients with GBM of the indicated subtypes; low 53BP1, bottom 50%; normal 53BP1, top 50%). G, 2-way contingency table indicating co-occurrence of TP53BP1 copy loss with TP53 alterations.

of apoptotic cells, relatively wild-type cells (Supplementary Fig. S2A).

To further characterize the role of 53BP1 in glioma therapeutic response, we silenced its expression with a panel of 11 different 53BP1 shRNAs (cloned into the pGIPZ lentiviral vector) in 2 different glioma cell lines, U251 and T98G (Supplementary Fig. S2B). We next selected 4 shRNAs with various knockdown efficiency (sh#11 ≈50%, sh#7 ≈80%, sh#9, and sh#1 ≈100%), when compared with the nontargeting shRNA (sh#12). The cells were then exposed to 10 Gy IR and the frequency of apoptotic cells was measured as sub-G_1 population by propidium iodide (PI) staining, 72 hours after treatment. As shown in Fig. 3B, in U251 cells, we observed an increase in the percentage of apoptotic cells that is proportional to the increase in 53BP1 silencing. Similarly to what we noticed in the RCAS glioma model and in the primary brain cell

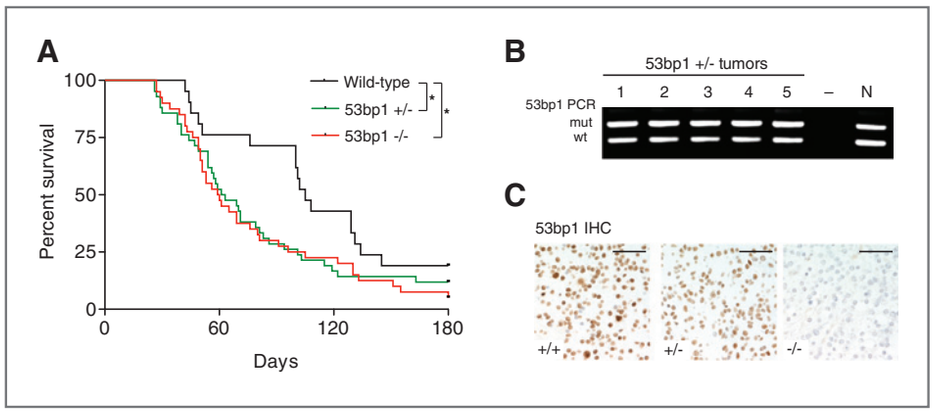

Figure 2. 53bp1 is a haploinsufficient tumor suppressor in a glioma mouse model. A, Kaplan–Meier survival curves of PDGF-induced gliomas in Nestin-tva mice of the indicated genotypes. B, genotyping PCR was conducted on genomic DNA extracted from *53bp1*+/− tumors. N, normal tissue; wt and mut, wild-type and mutant allele, respectively. C, IHC staining with anti-53bp1 antibody, conducted on gliomas of the indicated genotypes. Scale bars, 100 μm.

cultures, we observe no difference between control cells and the cells were 53BP1 expression was reduced by 50% (sh#11). Equivalent results were obtained in T98G cells (Supplementary Fig. S2C). Colony forming ability is considered the gold standard of radiosensitivity, therefore we then plated the cells at clonal density and exposed them to increasing doses of IR (0, 1, 2, 4, and 6 Gy). U251 cells with low 53BP1 levels (sh#7, sh#1, and sh#9) showed the lowest colony forming ability, as compared with either nontargeting shRNA (sh#12) or sh#11 (Fig. 3C).

To confirm these data and to broaden our studies on 53BP1 in glioma therapy response, U87MG (p53 wild-type), U251 (p53 mutant), and T98G (p53 mutant) cells were transduced with other 2 shRNAs that target 53BP1 mRNA, which both efficiently silenced 53BP1 protein level (Supplementary Fig. S2D). The cells were then exposed either to 10 Gy IR or treated with temozolomide (TMZ), of which various doses were used because of the variable sensitivity of the cell lines in the study (100 μmol/L for U87, 10 μmol/L for U251, and 250 μmol/L for T98G). As shown in Fig. 3D, *53BP1* gene silencing significantly increases IR sensitivity across all of these cell lines, whereas only slightly affects the percentage of apoptotic cells upon TMZ exposure. Moreover, *53BP1* gene silencing reduced the colony formation ability of the different cell lines, with the least sensitization in U87MG cells as compared with the U251 and T98G cells (Fig. 3E). We then measured the growth ability of the different glioma cells lines treated with different doses of TMZ. *53BP1* gene silencing increased the sensitivity to TMZ in U87MG cells (Fig. 3F, left) but not in U251 cells (Fig. 3F, right) and T98G cells (Supplementary Fig. S3).

These data show that although 53BP1 seems to be haploinsufficient in tumor suppression, this is not the case in therapy response. Moreover, 53BP1 function broadly protects all GBM cells from cell death in response to radiation, however, its role in TMZ response seems to be variable.

53BP1 silencing slows cell cycle and leads to accumulation of GBM cells in G_2 after IR exposure

IR and other DNA damaging agents create DSBs that are responsible for the initiation of the DDR and consequently the activation of cell-cycle checkpoints. Upon DNA damage exposure, GBM cells do not accumulate at the G_1 to S checkpoint, whereas predominantly arrest in the G_2 phase (15, 16). *53bp1*$^{-/-}$ mouse embryonic fibroblasts (MEF) have a minor S-phase checkpoint defect and prolonged G_2–M arrest after treatment with IR (17). To better understand the role of 53BP1 in glioma radiation response, we analyzed the cell-cycle checkpoints activation in GBM cells in which 53BP1 expression was silenced. As determined by PI staining, U251 cells accumulated in the G_2 phase at 24 hours after 10 Gy IR exposure. However, while the cells transduced with a control shRNA subsequently reenter the cell cycle, the cells in which 53BP1 was knocked-down failed to do so (Fig. 4A). To confirm that it is a true cell-cycle arrest (and not simply an increase in G_2 phase), we conducted a phospho-histone H3 (pH3) staining, commonly used to identify mitotic cells. The G_2–M checkpoint is rapidly activated in both control and 53BP1 knocked-down cells, as shown by the significant reduction of pH3 positive cells 3 hours post-IR (Fig. 4B). On the other hand, control cells progress into mitosis 24 hours after IR exposure (pH3+ cells $= 1.94 \pm 0.15$) whereas the cells in which 53BP1 expression has been silenced were still arrested in G_2 (pH3+ cells $= 0.47 \pm 0.14$; $P < 0.0001$, t test). It is worth noting that although at 48 hours the percentage of pH3+ cells in 53BP1 silenced cells is only slightly lower than control cells, because the number of cells in G_2 phase is much higher in 53BP1 silenced cells, the mitotic ratio (%pH3+ cells/% G_2–M cells) is still significantly lower than control cells ($P = 0.011$, t test). A similar prolonged arrest in G_2 phase, although with somewhat different kinetics (probably due to differences in cell-cycle length) was also observed in T98G and U87MG cells (Supplementary Fig. S4A and S4B).

To determine whether defects in the G_1 to S and S-phase checkpoints contribute to the differences in cell-cycle progression observed with 53BP1 knockdown, U251 cells were exposed to IR (10 Gy) and the percentage of cells in S-phase 16 hours posttreatment was measured by BrdUrd incorporation. Control cells showed only a moderate reduction (approximately 20%) in the percentage of BrdUrd-positive cells relative to mock-irradiated cells. In contrast, cells in which 53BP1 expression had been silenced, we detected an increase of BrdUrd-positive cells (from 40% to 100%, depending on the experiment; Supplementary Fig. S4C). This unexpected increase in the number of cells incorporating BrdUrd upon IR exposure might be due either to lengthened S-phase or a compromised S-phase arrest in 53BP1 defective cells. To explore these 2 hypotheses, we gave the cells a short pulse of BrdUrd (30′) and followed their progression through the cell cycle after exposure to IR. As

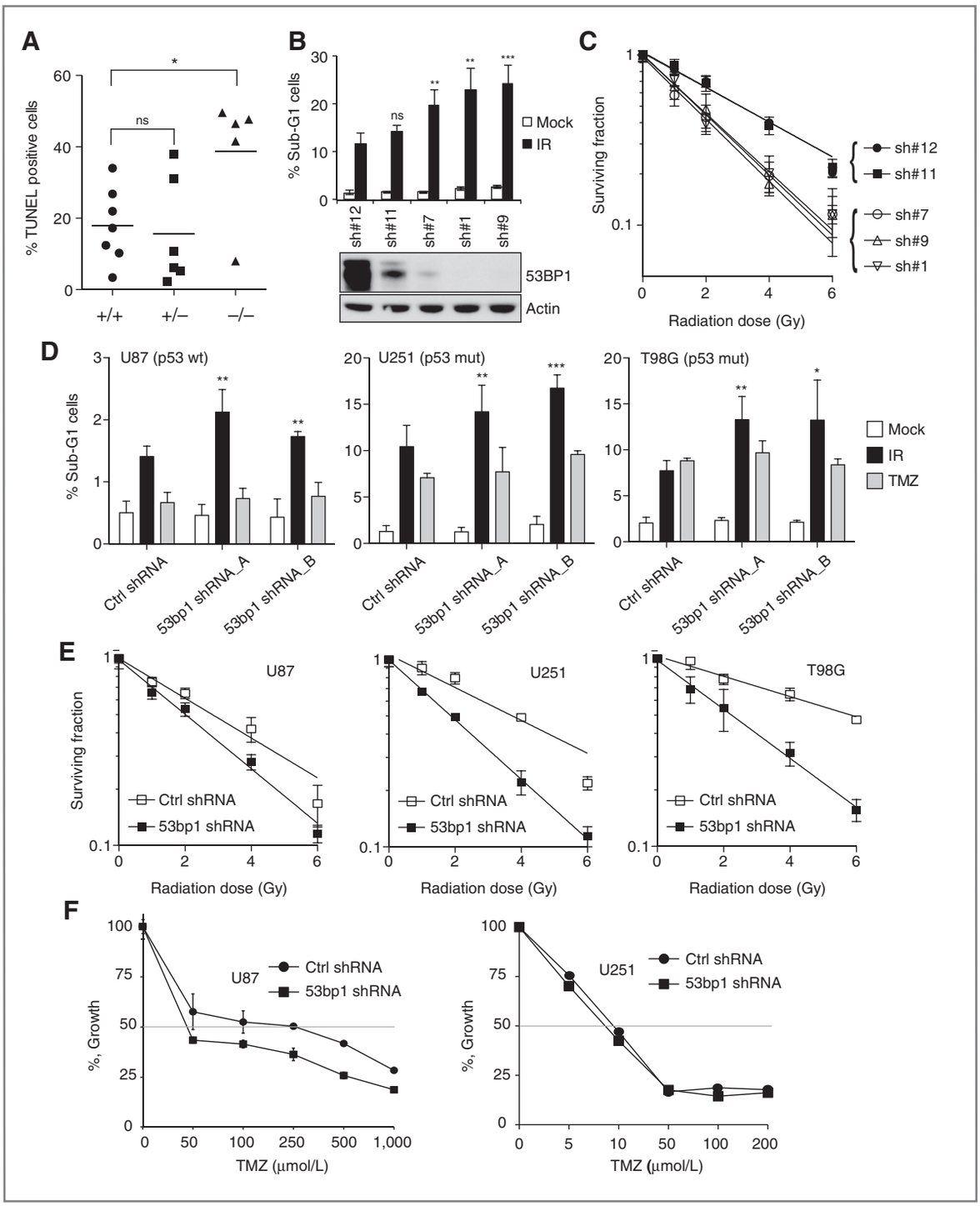

Figure 3. Efficient *53BP1* gene silencing sensitize GBM cell lines to DNA damaging therapy. A, percentage of TUNEL-positive glioma cells in tumor-bearing mice of the indicated genotypes; *t* test *, $P = 0.0272$. B, top, percentage of sub-G_1 cells in U251 cells transduced with the pGIPZ shRNAs. Bottom, Western blot analysis showing 53BP1 knockdown efficiency. C, colony formation assay of U251 cells transduced with the indicated pGIPZ shRNAs. Data are presented as mean ± SD of a representative of 2 independent experiments, each carried out in triplicate. D, percentage of sub-G_1 cells in U87MG, U251, and T98G glioma cell lines transduced with a pSuper control (ctrl) shRNA or 2 different shRNAs targeting 53bp1 upon IR or TMZ treatment. Data are presented as mean ± SD of a representative of either 2 or 3 independent experiments, each carried out in triplicate; *t* test: ***, $P < 0.001$; **, $P < 0.01$; *, $P < 0.05$. E, colony formation assay of the indicated cell lines transduced with ctrl shRNA or 53bp1 shRNA _A. F, cell counts of U87MG (left) and U251 (right) cell lines transduced with ctrl shRNA or 53bp1 shRNA _A at 3 days after TMZ exposure. Data are presented as mean ± SD of a representative of 2 independent experiments, each carried out in triplicate.

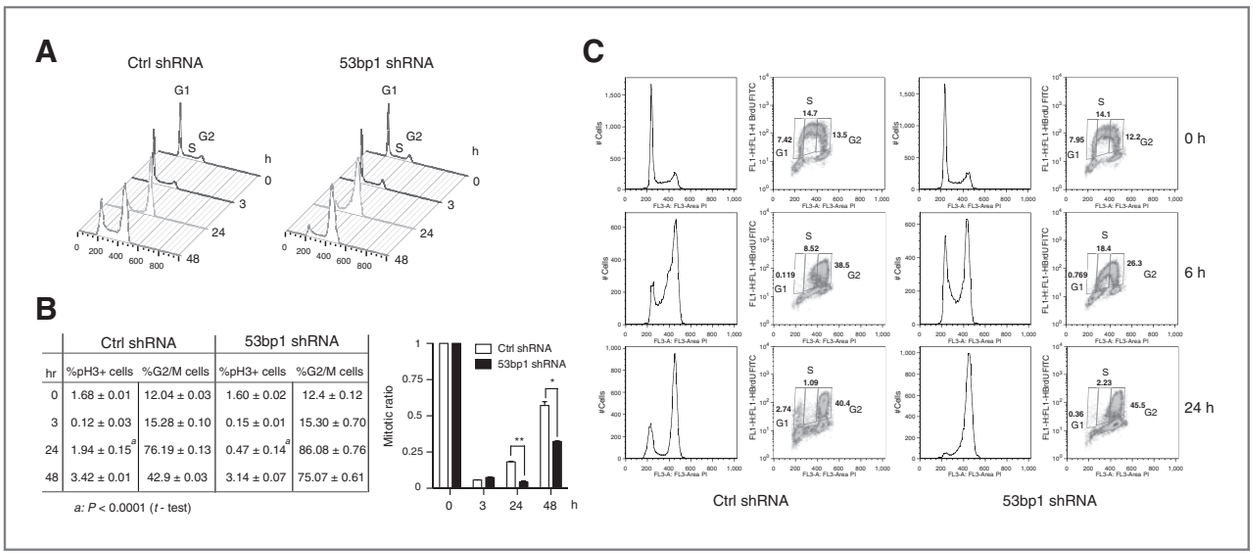

Figure 4. 53BP1 knockdown in GBM cells leads to a prolonged cell-cycle arrest after exposure to IR. A, cell-cycle analysis of U251 cells transduced with ctrl shRNA or 53bp1 shRNA _A at the indicated time point after IR exposure. B, left, table of the percentage of pH3 positive cells and percentage of cells in G_2–M phases of the cell-cycle at the indicated time point after 10 Gy of IR. Data are presented as mean ± SD of a representative of 2 independent experiments, each carried out in triplicate. Right, graph showing the mitotic ratio (%pH3 + cells/% G_2–M cells) of the data presented in left; *t* test: **, $P = 0.0046$; *, $P = 0.011$. C, cell-cycle analysis and BrdUrd staining in U251 cells exposed to a 30′ pulse of BrdUrd followed by 10 Gy of IR, and harvested at the indicated time-point after treatment.

shown in Fig. 4C, at 6 hours post-IR in the control cells, the BrdUrd-positive cells are mainly in late S and G_2 phases, having only 8.5% of BrdUrd-positive cells with a S-phase DNA content. In contrast, the 53bp1 shRNA cells lagged behind with 18.4% of BrdUrd-positive cells having an S-phase DNA content, suggesting that 53BP1 loss compromises the progression through S-phase after exposure to IR. Analogous to what we describe above, by 24 hours post-IR the control shRNA cells are reentering the cell cycle, whereas the 53bp1 shRNA cells were still arrested in G_2.

53BP1 is required for efficient nonhomologous end-joining in GBM cells

In eukaryotic cells, 2 major pathways are responsible for the repair of DSBs: the error-free homologous recombination (HR), that uses the intact sister chromatid as a template, and the error-prone NHEJ, with direct joining at the break site. Considering that many of the different effects in IR response observed in GBM cells could be related to defects in DSBs repair ability, we tested which of the 2 major DNA repair pathways (HR or NHEJ) was affected in GBM cells depleted for 53BP1.

To study HR, we took advantage of the DR-GFP reporter system (18), an assay that has been widely used to identify HR components of DNA repair. The DR-GFP reporter is made of 2 differentially mutated *GFP* gene repeats, with the upstream copy (SceGFP) containing a recognition site for the *I-Sce*I endonuclease and the downstream copy being a truncated inactive GFP fragment (iGFP; Fig. 5A). Expression of the *I-Sce*I enzyme leads to the creation of DSB in the upstream *GFP* gene copy; HR of the DSB will result in GFP+ cells that can be quantified by flow cytometry. U251 cells that were stably transduced with control shRNA and with 2 different shRNAs that target 53BP1, transiently transfected with the DR-GFP reporter and an expression plasmid encoding the *I-Sce*I endonuclease were analyzed by fluorescence-activated cell sorting (FACS) 24 hours later. As shown in the graph in Fig. 5A, no differences in HR efficiency between the 2 cell lines were detected.

We then analyzed NHEJ efficiency using the Pem1-Ad2-EGFP reporter assay (19, 20). This reporter construct consists of enhanced GFP (EGFP) coding sequence interrupted by the 2.4 kb *Pem1* gene intron in which it has been inserted the adenoviral exon Ad2, flanked at both sides by 2 *Hind*III restriction sites and 2 recognition sites for the *I-Sce*I endonuclease (in opposite directions). Digestion *in vitro* with the *Hind*III enzyme leads to the creation of cohesive ends, whereas digestion with *I-Sce*I leads to the formation of incompatible ends (Fig. 5B). Once the linearized plasmid is transduced into cells, it can be recircularized by NHEJ, the Pem1 intron is spliced out restoring EGFP expression and the GFP+ cells can be detected by FACS. Control shRNA and 53bp1 shRNA U251 cells were transduced with the linearized Pem1-Ad2-EGFP plasmid and analyzed by flow cytometry after 48 hours. An approximate 10% to 15% reduction of NHEJ efficiency was consistently detected in 53bp1 shRNA U251 cells using either *Hind*III or *I-Sce*I linearized plasmids (*t* test, $P = 0.0034$ and $P = 0.0018$, respectively; Fig. 5B). The Pem1-Ad2-EGFP reporter can also be transduced into the cells before the linearization and a DSB can be induced by cotransduction of the *I-SceI* endonuclease, parallel to the HR assay. Similar to that observed for the *in vitro* linearized plasmid, 53bp1 shRNA U251 cells showed significantly lower NHEJ efficiency ($P = 0.0069$, *t* test; Supplementary Fig. S5A).

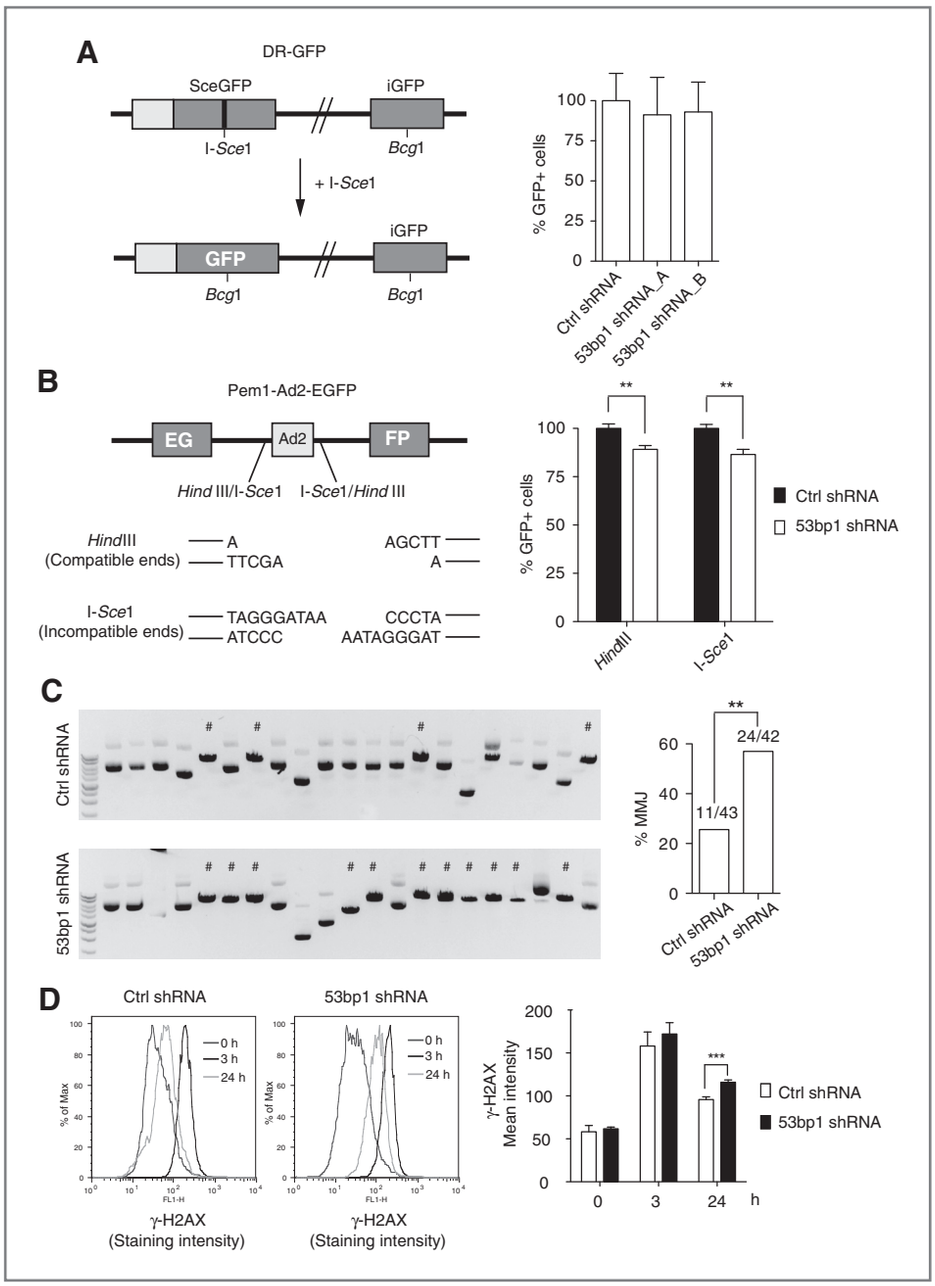

Figure 5. 53BP1 is required for an efficient NHEJ, whereas it represses alternative-NHEJ. A, left, schematic representation of the DR-GFP construct and assay used to measure HR efficiency (see text for details). Right, graph showing HR analysis conducted in U251 cells transduced with the indicated shRNAs. Data are presented as mean ± SD of 3 independent experiments. B, left, schematic representation of the Pem1-Ad2-EGFP construct and assay used to measure NHEJ efficiency (see text for details). Right, graph showing NHEJ analysis results, conducted in U251 cells transduced with ctrl shRNA or 53bp1 shRNA_A and with the Pem1-Ad2-EGFP previously linearized *in vitro* with either *Hind*III or *I-Sce*I enzymes. Data are presented as mean ± SD of 3 independent experiments, each done in either duplicate or triplicate; *t* test: **, $P < 0.005$. C, left, representative ethidium bromide stained agarose gels showing *Hind*III digestion products on the recovered plasmids from the NHEJ assay in B. #, MMJ events. Right, graph showing the percentage of MMJ in ctrl shRNA and 53bp1 shRNA U251 cells; Fisher exact test: **, $P = 0.0042$. D, DNA damage measured by γ-H2AX staining and analysis by flowcytometry of U251 cells after exposure to IR. Left, representative γ-H2AX staining intensity distribution. Right, graph of γ-H2AX mean intensity. Data are presented as mean ± SD of 3 independent experiments, each carried out in either duplicate or triplicate; *t* test: ***, $P = 0.0005$.

At least 2 molecularly distinct subpathways of NHEJ have been documented: a prominent "classic" pathway (C-NHEJ) and a less-understood "alternative" pathway (A-NHEJ), known also as microhomology-mediated end joining (MMEJ; ref. 21). While the C-NHEJ, normally may lead to small insertions or deletion at the junction site, the A-NHEJ always results in deletions (often with microhomology at the repair junction) and is frequently associated with chromosome translocation. One advantage of the Pem1-Ad2-EGFP reporter assay is that the repaired plasmids can be recovered from the cells and molecularly analyzed (20, 22). The *Hind*III-linearized substrate contains 4 bp compatible overhangs that represent microhomologous sequences. When these overhangs are used to mediate the repair event, the product now contains a single *Hind*III restriction site. As a consequence, the recovered Pem1-Ad2-EGFP plasmids can be analyzed by cleavage with the *Hind*III enzyme and by gel electrophoresis to measure the frequency of event that reconstitutes a single *Hind*III site ("microhomology-mediated junctions" or MMJ). Using this system, we found that *53BP1* gene silencing led to a significant increase of MMJ in U251 cells (Fig. 5C), with a frequency of 25.6% (11 of 43) in control shRNA cells and of 57.1% (24 of 42) in 53bp1 shRNA cells ($P = 0.0042$, Fisher

exact test). Similar results were obtained when the analysis of MMJ was conducted in T98G cells (Supplementary Fig. S5B).

We then asked whether the observed differences in NHEJ were sufficient to lead to a prolonged accumulation of DNA damage. The phosphorylated form of histone H2AX, commonly known as γ-H2AX, is routinely used as a marker of damaged DNA and of an activated DDR and can be measured by FACS. At 3 hours after IR exposure control and 53bp1 shRNA cells have similar level of γ-H2AX, whereas at 24 hours posttreatment 53BP1 knockdown cells have significantly higher level of γ-H2AX ($P = 0.0005$, t test; Fig. 5D). All together these data would suggest that 53BP1 is required for the repair of the DNA breaks induced by IR in glioma cells, and that the increase level of DNA damage might be responsible for the prolonged cell-cycle arrest and increased apoptosis observed in the 53bp1 shRNA cells.

53BP1 silencing potentiates radiosensitivity and extends survival in a GBM orthotopic model

Despite having a generally poor clinical outcome, IR and TMZ treatments are still the most effective therapies for patients with GBMs. Different strategies to increase radiation efficacy are currently under investigation in numerous laboratories and particular interest has been focused on the modulation of the DNA repair pathways (23). Although, 53BP1 is a tumor suppressor, because of its role in radiation response, we decided to investigate whether 53BP1 inhibition might be an effective addition to radiotherapy for GBM. *53bp1*$^{-/-}$ mice are extremely sensitive to IR and die of radiation poisoning even with local irradiation to the head (data not shown), we therefore used an orthotopic GBM model for long-term survival analysis. U251 cells were transduced with a TK-GFP-Luciferase reporter plasmid (TGL; ref. 24) to monitor tumor growth by bioluminescence measurements, and infected with either control shRNA or 53bp1 shRNA. These cells were then injected intracranially into athymic nude mice. Two weeks after injection half of the mice of each group (ctrl shRNA or 53bp1 shRNA), received local irradiation to the brain with a single dose of 6 Gy, analogous to what was used in a similar orthotopic model (16). In mice injected with control shRNA U251-TGL cells, bioluminescence analysis at 2 weeks postirradiation showed a nonsignificant difference (t test raw data $P = 0.158$ and normalized data $P = 0.3853$) in tumor progression between irradiated and nonirradiated group (Fig. 6A). In contrast, the mice injected with 53bp1 shRNA U251-TGL cells showed a highly significant reduction in tumor growth (raw data, $P = 0.0006$, t test; normalized data, $P = 0.005$). Consequently, survival analysis showed a significant extension of survival in the irradiated group of 53bp1 shRNA injected mice ($P = 0.0015$, log-rank test; Fig. 6B, right) but not in the control shRNA injected mice ($P = 0.0723$, log-rank test; Fig. 6B, left). Interestingly, when we compared 53BP1 expression by IHC in the "primary" tumors (that arise in the nonirradiated groups) with that of the "recurrent" tumors (that arise in the irradiated groups) we observed that, in the mice injected with the 53bp1 shRNA U251-TGL cells, the frequency of 53BP1 positive cells was significantly higher in the "recurrent" tumors ($P = 0.0002$, t test; Fig. 6C and D). No differences in 53BP1 staining were observed in the tumor derived from the control shRNA U251-TGL cells. A possible explanation of these data is that 53BP1 might have not been efficiently targeted in all cells by the shRNA expression, and considering that these cells survive better following IR, compared with the ones with no or low 53BP1 expression, they also might proficiently repopulate the tumor after IR exposure. As a consequence, a more efficient and homogenous silencing of 53BP1 would possibly lead to an even stronger radiosensitization of the tumors as a whole.

Discussion

In recent years, the DDR has emerged as an inducible barrier to tumorigenesis, and defects in elements of the DDR have been associated with different human cancers. Various studies had lately looked at 53BP1 protein expression and localization in different tumor types in human. As an example, in breast and lung tumors a subset of cases show aberrant 53BP1 activation, such as nuclear foci formation, however, others presented a reduction or a complete lack of its expression, that correlated with tumor stage (25, 26). A recent report shows that 53BP1 expression is reduced in a subset of basal-like/triple-negative breast cancers and in BRCA1/2-associated breast cancers, and among the triple-negative tumors, those that lack 53BP1 staining showed decreased metastasis-free survival (27).

Here, we present evidence that 53BP1 behaves as a haploinsufficient tumor suppressor in glioma. The *TP53BP1* gene, which encodes for the 53BP1 protein, is localized on 15q15-q21 and an analysis of the TCGA dataset for GBM showed single copy loss spanning this chromosomal region in approximately 20% of the patients, with a significant reduction of 53BP1 mRNA and protein expression. No homozygous loss was detected. These data are consistent with a previous array-CGH (aCGH) study conducted on a collection of 54 gliomas (including 31 GBMs), in which a subset of tumors showed 2 noncontiguous minimally deleted regions within chromosome 15q, mapping to 15q15.1 and 15q15.3 involving deletions of the *RAD51* gene and the *TP53BP1* gene (28). Most importantly, this study detected loss of a single gene copy of TP53BP1, both by aCGH and by real-time quantitative PCR analysis. Moreover, single-nucleotide polymorphisms (SNP) arrays showed LOH of the chromosomal region containing TP53BP1 in 55% (10 of 18) pediatric glioblastomas samples (29), indicating the relevance of our finding not only in the adult but also in pediatric glial tumors.

Our *in vivo* studies using the RCAS/PDGF glioma model ultimately confirmed the evidence of 53BP1 haploinsufficient role in glioma formation. Indeed, loss of a single copy of TP53BP1 was sufficient to accelerate PDGF-induced glioma in mice. Similarly, patients with GBM with lower 53BP1 levels show a somewhat poorer prognosis (Fig. 1C and Supplementary Fig. S1A). It is important to note that, as further discussed later, 53BP1 seems to have haploinsufficient activity in tumor formation but not in therapy response. Nevertheless, we speculate that both of these aspects are connected to 53BP1 role in DNA repair. While loss of a single *53BP1* gene copy would be

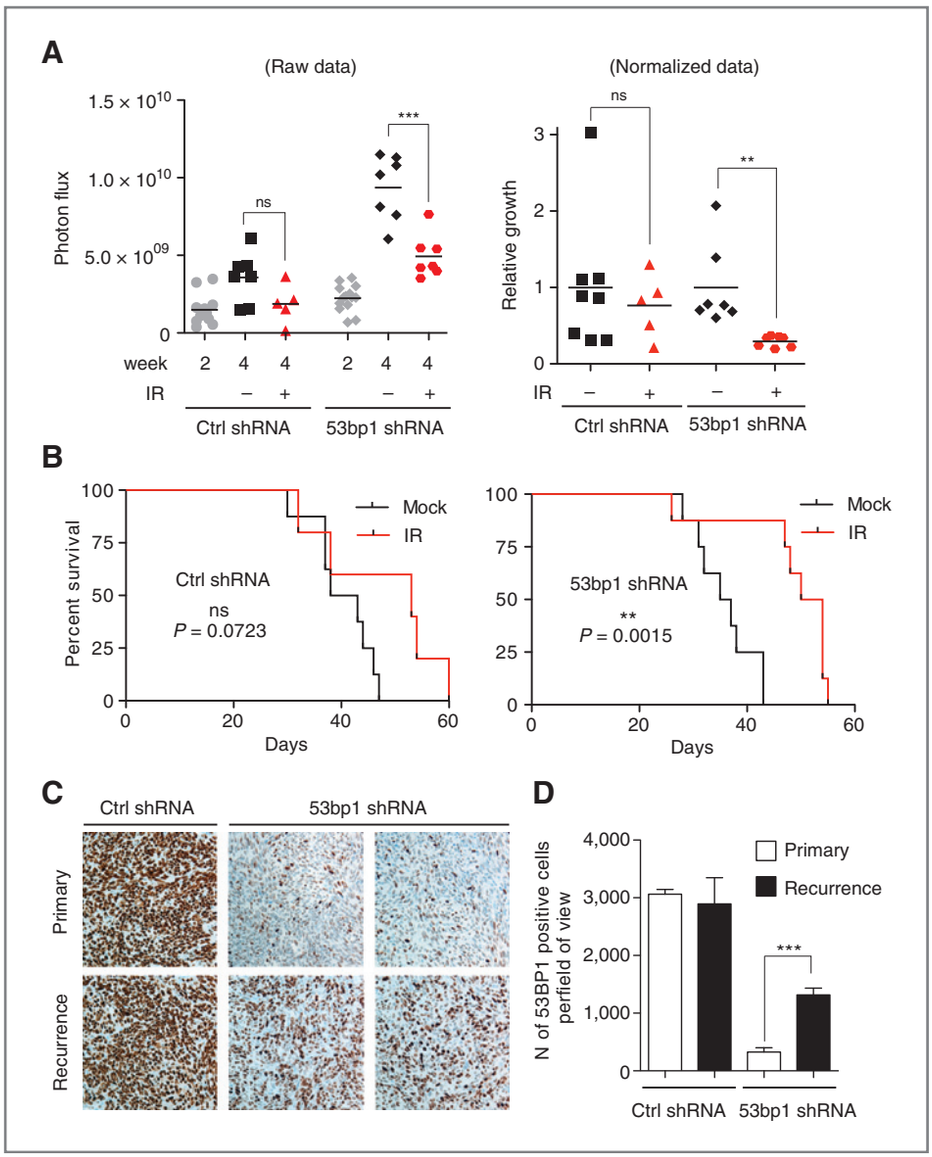

Figure 6. *53BP1* silencing increases radiosensitization *in vivo* in an orthotopic GBM mouse model. A, U251-TGL cells transduced with ctrl shRNA or 53bp1 shRNA_A were intracranial injected into nude mice. Two weeks after the injection the mice were divided in 2 groups, one of which was locally irradiated to the head with 6 Gy. The graph on the left shows the bioluminescence raw data at 2 and 4 weeks after injection; the graph on the right shows the normalized data for each tumor (photon flux at 4 weeks/photon flux at 2 weeks) presented as fold change over the average of the nonirradiated group; *t* test: ns, nonsignificant; ***, $P = 0.0006$ and **, $P = 0.005$. B, Kaplan–Meier survival curves of mice in A. C, representative IHC analysis of 53BP1 conducted on primary and recurrent gliomas generated in B. D, quantification of 53BP1-positive cells in gliomas as in C. Data are presented as mean ± SD of at least 3 independent tumors; *t* test: ***, $P = 0.0002$.

sufficient to sensitize the cells to oncogene induced DNA damage, a low persistent level of damage, this would not be the case for the acute DNA damage created by IR. In fact, it was previously shown that 53BP1 haploinsufficiency compromises genomic stability, although at lower extent than nullizigosity (4). However, we cannot exclude that this tumor suppressor activity might be linked to other not yet characterized role of 53BP1 in cellular transformation.

At present, a number of laboratories are exploring the possibility of manipulating the DDR to cause selective tumor cell death through mitotic catastrophe and as a possible therapeutic approach to improve the response to radiotherapy and chemotherapy in patients with GBM (6, 23). Here, we have shown that 53BP1 null mouse glioma cells, but not the heterozygous tumors, and human glioma cell lines in which 53BP1 was robustly silenced by shRNA, show higher level of sensitivity to IR, both *in vitro* and *in vivo*. 53BP1 levels seem to be critical for this radiosensitization, and a 50% reduction seems not to be sufficient to increase radiation sensitivity. This hypothesis would predict that only those patients in which 53BP1 expression decrease under a threshold level, or in which 53BP1 activity would be acutely inhibited, might have an improved therapy response.

Here, we propose that 53BP1 might represent one DDR component that would be worth targeting in patients with GBM in combination with radiotherapy. The fact that 20% of patients with GBM have lower levels of 53BP1, might give an enhanced therapeutic window, with limited normal tissue toxicity. The question is how effectively can 53BP1 function be inhibited. So far, it does not seem to have any enzymatic activity that eventually can be targeted. However, interfering with the proteins modifications necessary for 53BP1

recruitment to DNA damage foci would possibly lead to 53BP1 loss of function. Finally, delivery of siRNA targeting 53BP1, by polyethylenimine/siRNA or liposome/siRNA complexes, could be used as an alternative strategy, and it has been successfully used for other genes in GBM xenograft models (30–32).

Disclosure of Potential Conflicts of Interest

No potential conflicts of interest were disclosed.

Acknowledgments

The authors thank Robert Finney, Quancho Zhang, and Eletha Carbajal for technical support and Diane Domingo for part of the flow cytometric analysis. The authors also thank members of Dr. Holland's laboratory and Ranjit Bindra for discussion, Lisa Sevenich for the help in the TUNEL quantification, and Junjie Chen, Titia de Lange, Roderick Beijesbergen, and Scott H. Kaufmann for providing reagents.

Grant Support

The work of M. Squatrito was supported by a Fondazione Italiana Ricerca Cancro (FIRC) Fellowship, an American Brain Tumor Association (ABTA) Fellowship in memory of Justin Porter, and a Memorial Sloan-Kettering Brain Tumor Center Grant Award. F. Vanoli was supported by an American–Italian Cancer Foundation (AICF) Postdoctoral Research Fellowship.

The costs of publication of this article were defrayed in part by the payment of page charges. This article must therefore be hereby marked *advertisement* in accordance with 18 U.S.C. Section 1734 solely to indicate this fact.

Received January 5, 2012; revised July 26, 2012; accepted August 6, 2012; published OnlineFirst August 21, 2012.

References

1. Iwabuchi K, Bartel PL, Li B, Marraccino R, Fields S. Two cellular proteins that bind to wild-type but not mutant p53. Proc Natl Acad Sci U S A 1994;91:6098–102.
2. Iwabuchi K, Li B, Massa HF, Trask BJ, Date T, Fields S. Stimulation of p53-mediated transcriptional activation by the p53-binding proteins, 53BP1 and 53BP2. J Biol Chem 1998;273:26061–8.
3. Noon AT, Goodarzi AA. 53BP1-mediated DNA double strand break repair: insert bad pun here. DNA Repair (Amst) 2011;10: 1071–6.
4. Ward IM, Difilippantonio S, Minn K, Mueller MD, Molina JR, Yu X, et al. 53BP1 cooperates with p53 and functions as a haploinsufficient tumor suppressor in mice. Mol Cell Biol 2005;25:10079–86.
5. Morales JC, Franco S, Murphy MM, Bassing CH, Mills KD, Adams MM, et al. 53BP1 and p53 synergize to suppress genomic instability and lymphomagenesis. Proc Natl Acad Sci U S A 2006;103:3310–5.
6. Squatrito M, Brennan CW, Helmy K, Huse JT, Petrini JH, Holland EC. Loss of ATM/Chk2/p53 pathway components accelerates tumor development and contributes to radiation resistance in gliomas. Cancer Cell 2010;18:619–29.
7. Cerami E, Gao J, Dogrusoz U, Gross BE, Sumer SO, Aksoy BA, et al. The cBio cancer genomics portal: an open platform for exploring multidimensional cancer genomics data. Cancer Discov 2012;2:401–4.
8. Holland EC, Hively WP, DePinho RA, Varmus HE. A constitutively active epidermal growth factor receptor cooperates with disruption of G_1 cell-cycle arrest pathways to induce glioma-like lesions in mice. Genes Dev 1998;12:3675–85.
9. Brummelkamp TR, Fabius AW, Mullenders J, Madiredjo M, Velds A, Kerkhoven RM, et al. An shRNA barcode screen provides insight into cancer cell vulnerability to MDM2 inhibitors. Nat Chem Biol 2006;2: 202–6.
10. The Cancer Geneome Atlas Network. Comprehensive genomic characterization defines human glioblastoma genes and core pathways. Nature 2008;455:1061–8.
11. Brennan C, Momota H, Hambardzumyan D, Ozawa T, Tandon A, Pedraza A, et al. Glioblastoma subclasses can be defined by activity among signal transduction pathways and associated genomic alterations. PLoS ONE 2009;4:e7752.
12. Verhaak RG, Hoadley KA, Purdom E, Wang V, Qi Y, Wilkerson MD, et al. Integrated genomic analysis identifies clinically relevant subtypes of glioblastoma characterized by abnormalities in PDGFRA, IDH1, EGFR, and NF1. Cancer Cell 2010;17:98–110.
13. Holland EC, Hively WP, Gallo V, Varmus HE. Modeling mutations in the G_1 arrest pathway in human gliomas: overexpression of CDK4 but not loss of INK4a-ARF induces hyperploidy in cultured mouse astrocytes. Genes Dev 1998;12:3644–9.
14. Shih AH, Dai C, Hu X, Rosenblum MK, Koutcher JA, Holland EC. Dose-dependent effects of platelet-derived growth factor-B on glial tumorigenesis. Cancer Res 2004;64:4783–9.
15. Hirose Y, Berger MS, Pieper RO. p53 effects both the duration of G_2/M arrest and the fate of temozolomide-treated human glioblastoma cells. Cancer Res 2001;61:1957–63.
16. Mir SE, De Witt Hamer PC, Krawczyk PM, Balaj L, Claes A, Niers JM, et al. *In silico* analysis of kinase expression identifies WEE1 as a gatekeeper against mitotic catastrophe in glioblastoma. Cancer Cell 2010;18:244–57.
17. Ward IM, Minn K, van Deursen J, Chen J. p53 Binding protein 53BP1 is required for DNA damage responses and tumor suppression in mice. Mol Cell Biol 2003;23:2556–63.
18. Pierce AJ, Johnson RD, Thompson LH, Jasin M. XRCC3 promotes homology-directed repair of DNA damage in mammalian cells. Genes Dev 1999;13:2633–8.
19. Patel AG, Sarkaria JN, Kaufmann SH. Nonhomologous end joining drives poly(ADP-ribose) polymerase (PARP) inhibitor lethality in homologous recombination-deficient cells. Proc Natl Acad Sci U S A 2011;108:3406–11.
20. Seluanov A, Mittelman D, Pereira-Smith OM, Wilson JH, Gorbunova V. DNA end joining becomes less efficient and more error-prone during cellular senescence. Proc Natl Acad Sci U S A 2004;101: 7624–9.
21. McVey M, Lee SE. MMEJ repair of double-strand breaks (director's cut): deleted sequences and alternative endings. Trends Genet 2008;24:529–38.
22. Fattah F, Lee EH, Weisensel N, Wang Y, Lichter N, Hendrickson EA. Ku regulates the non-homologous end joining pathway choice of DNA double-strand break repair in human somatic cells. PLoS Genet 2010;6:e1000855.
23. Squatrito M, Holland EC. DNA damage response and growth factor signaling pathways in gliomagenesis and therapeutic resistance. Cancer Res 2011;71:5945–9.
24. Ponomarev V, Doubrovin M, Serganova I, Vider J, Shavrin A, Beresten T, et al. A novel triple-modality reporter gene for whole-body fluorescent, bioluminescent, and nuclear noninvasive imaging. Eur J Nucl Med Mol Imaging 2004;31:740–51.
25. Bartkova J, Horejsi Z, Sehested M, Nesland JM, Rajpert-De Meyts E, Skakkebaek NE, et al. DNA damage response mediators MDC1 and 53BP1: constitutive activation and aberrant loss in breast and lung cancer, but not in testicular germ cell tumours. Oncogene 2007;26: 7414–22.
26. Nuciforo PG, Luise C, Capra M, Pelosi G, d'Adda di Fagagna F. Complex engagement of DNA damage response pathways in human cancer and in lung tumor progression. Carcinogenesis 2007; 28:2082–8.
27. Bouwman P, Aly A, Escandell JM, Pieterse M, Bartkova J, van der Gulden H, et al. 53BP1 loss rescues BRCA1 deficiency and is associated with triple-negative and BRCA-mutated breast cancers. Nat Struct Mol Biol 2010;17:688–95.

28. Bredel M, Bredel C, Juric D, Harsh GR, Vogel H, Recht LD, et al. High-resolution genome-wide mapping of genetic alterations in human glial brain tumors. Cancer Res 2005;65:4088–96.
29. Qu HQ, Jacob K, Fatet S, Ge B, Barnett D, Delattre O, et al. Genome-wide profiling using single-nucleotide polymorphism arrays identifies novel chromosomal imbalances in pediatric glioblastomas. Neuro Oncol 2010;12:153–63.
30. Grzelinski M, Urban-Klein B, Martens T, Lamszus K, Bakowsky U, Hobel S, et al. RNA interference-mediated gene silencing of pleiotrophin through polyethylenimine-complexed small interfering RNAs *in vivo* exerts antitumoral effects in glioblastoma xenografts. Hum Gene Ther 2006;17:751–66.
31. Kato T, Natsume A, Toda H, Iwamizu H, Sugita T, Hachisu R, et al. Efficient delivery of liposome-mediated MGMT-siRNA reinforces the cytotoxity of temozolomide in GBM-initiating cells. Gene Ther 2010;17:1363–71.
32. Hendruschk S, Wiedemuth R, Aigner A, Topfer K, Cartellieri M, Martin D, et al. RNA interference targeting survivin exerts antitumoral effects *in vitro* and in established glioma xenografts *in vivo*. Neuro Oncol 2011;13:1074–89.